On the influence of curvature on transmission conditions

Hélène Barucq[1], Martin J. Gander[2], and Yingxiang Xu[3]

1 Introduction

Domain decomposition methods are both highly successful parallel solvers and also important modeling tools, since problems in subdomains can be treated by adapted methods to the physics in each subdomain. Subdomain boundaries are therefore rarely straight lines. The focus of this paper is to study the influence of curvature on transmission conditions used in optimized Schwarz methods. For straight interfaces and simple geometries, optimized interface conditions are typically determined using Fourier analysis, see for example [4] and references therein. Asymptotically, these optimized conditions are still valid for curved interfaces, as shown in [5, 6]. Since however the curvature is the most important information for a smooth curve, we want to study in this paper if and how the interface curvature influences the constants in the optimized parameters.

We consider the model problem

$$(\Delta - \eta)u = f, \quad \text{on } \Omega = \mathbb{R}^2,\ \eta > 0, \tag{1}$$

and we require the solution to decay at infinity. As shown in Fig. 1 on the left, we decompose Ω into two overlapping subdomains $\Omega_1 = (-\infty, a(y)) \times \mathbb{R}$ and $\Omega_2 = (b(y), \infty) \times \mathbb{R}$, where Γ_1 given by $a(y)$ and Γ_2 given by $b(y)$ are smooth curves satisfying $a(y) \geq b(y)$. A general parallel Schwarz algorithm is then given by

$$\begin{aligned} (\Delta - \eta)u_i^n &= f && \text{in } \Omega_i, \\ \mathscr{B}_i(u_i^n) &= \mathscr{B}_i(u_j^{n-1}) && \text{on } \Gamma_i,\ 1 \leq i \neq j \leq 2, \end{aligned} \tag{2}$$

where $\mathscr{B}_i, i = 1,2$, are transmission conditions to be chosen. If $\mathscr{B}_i$, $i = 1,2$ are chosen as $\partial_{n_i} + DtN_i$, with DtN_i the Dirichlet to Neumann operators, the iterates will converge in two steps [4]. These operators are however non-local, and thus difficult to use in practice. Therefore, local approximations are used in optimized Schwarz methods. We study in what follows such local approximations, obtained by microlocal analysis, and by studying a circular model problem, with the goal to investigate how the curvature influences these approximations.

[1] Hélène Barucq, MAGIQUE-3D (INRIA Bordeaux - Sud-Ouest) INRIA-CNRS-Université de Pau et des Pays de l'Adour, BP 1155, F64013 PAU, France, e-mail: helene.barucq@inria.fr .[2] Martin J. Gander, Section de Mathématiques, Université de Genève, 2-4 rue du Lièvre, CP 64, 1211 Genève 4, Suisse, e-mail: Martin.Gander@unige.ch .[3] Yingxiang Xu, School of Mathematics and Statistics, Northeast Normal University, Changchun 130024, China, e-mail: yxxu@nenu.edu.cn, partly supported by NSFC-11201061 and CPSF-2012M520657.

2 Transmission conditions based on micro-local analysis

Micro-local analysis is a well established technique for the design and study of absorbing boundary conditions, where it is used to approximate the *DtN*, see [2] and references therein. We use in this section micro-local analysis to develop and analyze transmission conditions. As in [2], we consider local coordinates composed by the curvilinear abscissa s and the variable r along the normal direction. In these local coordinates, the model problem (1) can be rewritten as

$$\mathscr{L}u := \partial_{rr}u + \frac{\kappa}{h}\partial_r u + \frac{1}{h}\partial_s(\frac{\partial_s u}{h}) - \eta u = f, \tag{3}$$

where $\kappa = \kappa(s)$ is the curvature of the curve Γ_i at the parameter s, and $h = h(r,s) = 1 + r\kappa(s)$. The symbol of the operator $\mathscr{L}$ is given by

$$\hat{\mathscr{L}} = \partial_{rr} + \frac{\kappa}{h}\partial_r + \frac{i}{h}\partial_s(\frac{1}{h})\xi - \frac{1}{h^2}\xi^2 - \eta. \tag{4}$$

A pseudodifferential operator $\mathscr{P}$ is defined by $\mathscr{P}u(x) := \int e^{ix\cdot\xi} p(x,\xi)\hat{u}(\xi)d\xi$, provided its symbol $p(x,\xi) \in S^m$, i.e. for every compact set K in $\mathbb{R}^n$ and for every α,β there exists $c = c(\alpha,\beta,K)$ s.t. for all $(x,\xi) \in K \times \mathbb{R}^n$, $|\partial_\xi^\alpha D_x^\beta p(x,\xi)| \leq c(1+|\xi|)^{m-|\alpha|}$. Based on the Nirenberg's factorization theorem, there exist two classical pseudo-differential operators Λ^- and Λ^+ of order $+1$, depending smoothly on r, such that

$$\mathscr{L}u = (\partial_r + \Lambda^-)(\partial_r + \Lambda^+)u, \tag{5}$$

which can be expanded as

$$\mathscr{L}u = \partial_{rr}u + (\Lambda^- + \Lambda^+)\partial_r u + \mathrm{op}(\partial_r\lambda^+)u + \Lambda^-\Lambda^+ u, \tag{6}$$

where $\mathrm{op}(\partial_r\lambda^+)$ is the operator whose symbol is $\partial_r\lambda^+$. In (5) and (6), the symbol '$=$' must be interpreted as equal up to a C^∞-regularizing operator, since the symbols of Λ^+ and Λ^- are explicitely defined by the factorization process up to a symbol in

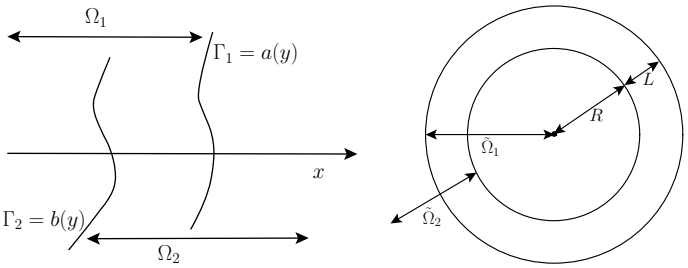

Fig. 1 An arbitrary domain decomposition with curved interfaces (left) and a circular domain decomposition (right)

$S^{-\infty}$. Identifying (3) and (6) we get

$$\Lambda^- + \Lambda^+ = \frac{\kappa}{h}, \quad \mathrm{op}(\partial_r \lambda^+) + \Lambda^- \Lambda^+ = \frac{1}{h}\partial_s(\frac{\partial_s}{h}) - \eta. \tag{7}$$

Due to the integral representation formula of pseudo-differential operators, the operators Λ^- and Λ^+ are determined by their symbols. Using the calculus of pseudo-differential operators, system (7) can be written at the symbol level,

$$\lambda^- + \lambda^+ = \frac{\kappa}{h}, \quad \sum_{\alpha=0}^{+\infty} \frac{(-i)^\alpha}{\alpha!} \partial_\xi^\alpha \lambda^- \partial_s^\alpha \lambda^+ + \partial_r \lambda^+ = -\eta - h^{-2}\xi^2 + \frac{i}{h}\partial_s(\frac{1}{h})\xi, \tag{8}$$

where $\lambda^\pm \sim \sum_{j=-1}^{+\infty} \lambda_{-j}^\pm$ are the symbols of $\Lambda^\pm$. The goal is now to determine the symbols λ^- and λ^+: from the first equation in (8), we get

$$\lambda_{-j}^- + \lambda_{-j}^+ = 0, \text{ if } j \neq 0 \text{ and } \lambda_0^- + \lambda_0^+ = \frac{\kappa}{h}. \tag{9}$$

By identifying the homogeneous symbols of highest degree, we obtain

$$\lambda_1^- \lambda_1^+ = -h^{-2}\xi^2 - \eta, \tag{10}$$

where η is considered to be an operator of order 2, see Section 3 of [2] for details. Therefore, we have

$$\lambda_1^+ = \sqrt{h^{-2}\xi^2 + \eta} \quad \text{and} \quad \lambda_1^- = -\sqrt{h^{-2}\xi^2 + \eta}. \tag{11}$$

Going further with the identification of the homogeneous symbols of the next higher degree, we find a relation between the unknowns λ_0^- and λ_0^+,

$$\lambda_1^- \lambda_0^+ + \lambda_0^- \lambda_1^+ - i\partial_\xi \lambda_1^- \partial_s \lambda_1^+ + \partial_r \lambda_1^+ = \frac{i}{h}\partial_s(\frac{1}{h})\xi. \tag{12}$$

Eliminating λ_1^- and λ_0^-, we get

$$\lambda_0^+ = \frac{1}{2\lambda_1^+}(\frac{\kappa}{h}\lambda_1^+ + i\partial_\xi \lambda_1^+ \partial_s \lambda_1^+ + \partial_r \lambda_1^+ - \frac{i}{h}\partial_s(\frac{1}{h})\xi). \tag{13}$$

We can derive a recursive formula from similar relations for lower degrees of homogeneity. First, we rewrite the left-hand side of the second equation in (8) as

$$\sum_{\alpha=0}^{+\infty} \frac{(-i)^\alpha}{\alpha!} \sum_{j=-1}^{+\infty} \partial_\xi^\alpha \lambda_{-j}^- \sum_{k=-1}^{+\infty} \partial_s^\alpha \lambda_{-k}^+ + \sum_{l=-1}^{+\infty} \partial_r \lambda_{-l}^+. \tag{14}$$

Since $\partial_\xi^\alpha \lambda_{-j}^- \partial_s^\alpha \lambda_{-k}^+ \in S^{-(j+k+\alpha)}$, the homogeneous part of degree $-m$ in (14) for any non-negative integer m is

$$\sum_{\alpha=0}^{m+2}\frac{(-i)^\alpha}{\alpha!}\sum_{\substack{j+k=m-\alpha,\\ j\geq -1,k\geq -1}}\partial_\xi^\alpha\lambda_{-j}^-\partial_s^\alpha\lambda_{-k}^+ + \partial_r\lambda_{-m}^+.$$

Identifying symbols of the same homogeneity in (8) leads to

$$\sum_{\alpha=0}^{m+2}\frac{(-i)^\alpha}{\alpha!}\sum_{\substack{j+k=m-\alpha,\\ j\geq -1,k\geq -1}}\partial_\xi^\alpha\lambda_{-j}^-\partial_s^\alpha\lambda_{-k}^+ + \partial_r\lambda_{-m}^+ = 0.$$

Using that $\lambda_{-m-1}^- = -\lambda_{-m-1}^+$, from the previous equation, the symbol λ_{-m-1}^+ for $m\geq 0$ can be recursively expressed from homogeneous symbols of higher order by

$$\lambda_{-m-1}^+ = \frac{1}{2\lambda_1^+}\Big(\sum_{\substack{j+k=m,\\ j\geq 0,k\geq 0}}\lambda_{-j}^-\lambda_{-k}^+ + \sum_{\alpha=1}^{m+2}\frac{(-i)^\alpha}{\alpha!}\sum_{\substack{j+k=m-\alpha,\\ j\geq -1,k\geq -1}}\partial_\xi^\alpha\lambda_{-j}^-\partial_s^\alpha\lambda_{-k}^+ + \partial_r\lambda_{-m}^+\Big). \tag{15}$$

Let ℓ be a positive integer, and μ be the symbol of the pseudo-differential operator $\mathrm{op}(\mu)$ defined on $\Gamma_i\times(-\delta,\delta)$, $i=1,2$, such that $\sum_{-1\leq j\leq p}\lambda_{-j}^+ - \mu$ is of order $(1/\sqrt{\eta})^{\ell-1}$ for all sufficiently large p. Denoting by $\tilde{\mu}$ the symbol defined on $\Gamma_i, i=1,2$ by $\tilde{\mu} := \mu|_{r=0}$, and choosing as transmission condition $\mathscr{B}_i = \partial_{n_i} + \mathrm{op}(\tilde{\mu})$ on Γ_i, we obtain the MATCs (Micro-local Analysis based Transmission Conditions) of order $\ell/2$ as

$$\mathscr{B}_i = \partial_{n_i} + \mathrm{op}\Big(\sum_{-1\leq j\leq \ell-2}\lambda_{-j}^+\Big), \quad \text{on } \Gamma_i,\ i=1,2. \tag{16}$$

From (15), note that λ_{-m-1}^+ still contains the term $\lambda_1^+ = \sqrt{h^{-2}\xi^2+\eta}$, and thus results in non-local transmission conditions. To obtain local transmission conditions, we use a Taylor expansion in ξ of the symbols λ_{-j}^+, $-1\leq j\leq 2$ to the order shown as index in the parentheses below, and obtain the following MATCs:

MATC1 $\quad \mathscr{B}_i(u) = \partial_{n_i}u + \mathrm{op}((\lambda_1^+)_0)u = \partial_{n_i}u + \sqrt{\eta}u;$

MATC2 $\quad \mathscr{B}_i(u) = \partial_{n_i}u + \mathrm{op}((\lambda_1^+)_0 + (\lambda_0^+)_0)u = \partial_{n_i}u + (\sqrt{\eta}+\frac{\kappa}{2})u;$

MATC3 $\quad \mathscr{B}_i(u) = \partial_{n_i}u + \mathrm{op}(\sum_{j=-1}^{2}(\lambda_{-j}^+)_0)u = \partial_{n_i}u + (\sqrt{\eta}+\frac{\kappa}{2} - \frac{\kappa^2}{8\sqrt{\eta}} + \frac{\kappa^3+\frac{d^2}{ds^2}\kappa(s)}{8\eta})u;$

MATC4 $\quad \mathscr{B}_i(u) = \partial_{n_i}u + \mathrm{op}(\sum_{j=-1}^{1}(\lambda_{-j}^+)_1)u = \partial_{n_i}u + (\sqrt{\eta}+\frac{\kappa}{2} - \frac{1}{8}\frac{\kappa^2}{\sqrt{\eta}})u - \frac{\frac{d}{ds}\kappa(s)}{2\eta}\partial_s u;$

MATC5 $\quad \mathscr{B}_i(u) = \partial_{n_i}u + \mathrm{op}((\lambda_1^+)_2)u = \partial_{n_i}u + \sqrt{\eta}u - \frac{1}{2\sqrt{\eta}}\partial_s^2 u;$

MATC6
$$\begin{aligned}\mathscr{B}_i(u) = {}& \partial_{n_i}u + \mathrm{op}(\textstyle\sum_{j=-1}^{2}(\lambda_{-j}^+)_{-2})u = \partial_{n_i}u + (\sqrt{\eta}+\frac{\kappa}{2} - \frac{1}{8}\frac{\kappa^2}{\sqrt{\eta}} + \frac{1}{8}\frac{\kappa^3+\frac{d^2}{ds^2}\kappa(s)}{\eta})u\\ &+(\frac{\frac{d}{ds}\kappa(s)}{2\eta} - \frac{13}{8}\frac{\kappa(s)\frac{d}{ds}\kappa(s)}{\eta^{\frac{3}{2}}})\partial_s u - (\frac{1}{2\sqrt{\eta}} - \frac{1}{2}\frac{\kappa}{\eta} + \frac{13}{16}\frac{\kappa^2}{\eta^{\frac{3}{2}}} - \frac{7}{8}\frac{2\kappa^3+\frac{d^2}{ds^2}\kappa(s)}{\eta^2})\partial_s^2 u,\end{aligned}$$

where the MATC1–3 are of order 0, MATC4 is of order 1, and MATC5 and MATC6 are of order 2. Note how the curvature $\kappa(s)$ enters these transmission conditions.

3 Transmission conditions based on a circular model problem

For optimized Schwarz methods, transmission conditions are often analyzed and optimized for a model problem, see [4]. Following this principle, we consider a circular decomposition of the domain $\Omega = \mathbb{R}^2$ as shown in Fig. 1 on the right,

$$\tilde{\Omega}_1 = \{(x,y)|\sqrt{x^2+y^2} < R_1 = R+L\}, \quad \tilde{\Omega}_2 = \{(x,y)|R_2 = R < \sqrt{x^2+y^2} < \infty\}.$$

In this setting, the curvature of the interface enters naturally, $\kappa(s) = 1/R$. Using polar coordinates, a general Schwarz algorithm for this decomposition is

$$\begin{aligned} \partial_{rr}u_i^n + \tfrac{1}{r}\partial_r u_i^n + \tfrac{1}{r^2}\partial_{\theta\theta}u_i^n - \eta u_i^n = f \quad & \text{in } \tilde{\Omega}_i, \\ \mathscr{B}_i(u_i^n) = \mathscr{B}_i(u_j^{n-1}) \quad & \text{on } r = R_i,\ 1 \le i \ne j \le 2. \end{aligned} \tag{17}$$

In the classical Schwarz algorithm, one uses for $\mathscr{B}_i$ the identity operator in (17). Using Fourier series in the angular variable, we obtain after a short calculation for the convergence factor ρ_{cla} in this case (for details of such calculations, see [3])

$$\rho_{cla} = \rho_{cla}(k,R,L,\eta) := \frac{I_k(\sqrt{\eta}R)}{K_k(\sqrt{\eta}R)}\frac{K_k(\sqrt{\eta}(R+L))}{I_k(\sqrt{\eta}(R+L))}, \quad \forall k \in \mathbb{R}, \tag{18}$$

where $I_k(\cdot)$ and $K_k(\cdot)$ are the modified Bessel functions of the first (exponentially increasing) and the second kind (exponentially decreasing), see [1]. Hence, for an overlap $L > 0$, the classical Schwarz algorithm converges, with the asymptotic estimate

$$\sup_{k_{\min} \le k \le k_{\max}} \rho_{cla} = 1 - G_{min}L + O(L^2), \quad G_{min} = \frac{1}{RI_{k_{min}}(\sqrt{\eta}R)K_{k_{min}}(\sqrt{\eta}R)},$$

where $k_{\min}$ and k_{max} denote the estimates of the lowest and highest relevant numerical frequencies respectively. If there is no overlap, the method does not converge.

Optimized Schwarz methods are based on linear operators S_i, $i = 1,2$ along the interface, here in the θ direction, with symbols σ_i, and $\mathscr{B}_i(u) = \partial_r u - S_i u$ in (17). This results in methods with convergence factors $\rho_{opt}(k,L,R,\eta,\sigma_1,\sigma_2)$ given by (for details, see [3])

$$\rho_{opt} = \frac{\frac{\partial_r K_k(\sqrt{\eta}r)}{K_k(\sqrt{\eta}r)} + \sigma_1(k)}{\frac{\partial_r I_k(\sqrt{\eta}r)}{I_k(\sqrt{\eta}r)} + \sigma_1(k)}\Big|_{r=R+L} \cdot \frac{\frac{\partial_r I_k(\sqrt{\eta}r)}{I_k(\sqrt{\eta}r)} - \sigma_2(k)}{\frac{\partial_r K_k(\sqrt{\eta}r)}{K_k(\sqrt{\eta}r)} - \sigma_2(k)}\Big|_{r=R} \cdot \rho_{cla}. \tag{19}$$

We can see from (19) that the optimal choice for which ρ_{opt} vanishes is $\sigma_1(k) = -\frac{\partial_r K_k(\sqrt{\eta}r)}{K_k(\sqrt{\eta}r)}|_{r=R+L}$ and $\sigma_2(k) = \frac{\partial_r I_k(\sqrt{\eta}r)}{I_k(\sqrt{\eta}r)}|_{r=R}$, again the symbol of the non-local DtN operator. Optimized Schwarz methods use local approximations of the form

$$\sigma_i(k) = p_i + q_i k^2, \quad i = 1,2, \tag{20}$$

and determine p_i, q_i such that the convergence factor $\rho(k,L,R,\eta,p_1,p_2,q_1,q_2)$ is small. These transmission conditions are then easy to use and inexpensive. Simple approximations are obtained by Taylor expansion of the approximation $\sqrt{\eta+k^2/R_i^2}$ of the optimal symbol: T0 (Taylor of order zero) is given by $p_1=p_2=\sqrt{\eta}$, $q_1=q_2=0$, and leads with the estimate $k_{max}=\frac{\pi R}{h}$, where h is the mesh size, to the asymptotic convergence factor bounds $1-4\sqrt{2}\eta^{\frac{1}{4}}\sqrt{h}+O(h)$ with overlap $L=h$, and $1-4\sqrt{\eta}\pi^{-1}h+O(h^2)$ without overlap (still convergent!). T2 (Taylor of order two) is obtained with $p_i=\sqrt{\eta}$, $q_i=\frac{1}{2\sqrt{\eta}R_i}$, $i=1,2$, and leads to the bounds $1-8\eta^{\frac{1}{4}}\sqrt{h}+O(h)$ with overlap $L=h$, and $1-8\sqrt{\eta}\pi^{-1}h+O(h^2)$ without overlap. It is interesting to note that the curvature $1/R$ does not play a role in the asymptotic convergence factor estimates!

Optimized transmission conditions are based on minimizing the maximum of the convergence factor: let $C_{\text{OO0}}=\{p_1=p_2>0,q_1=q_2=0\}$, $C_{\text{OO2}}=\{p_1=p_2>0,q_1=q_2>0\}$ and $C_{\text{2-sided}}=\{p_1>0,p_2>0,q_1=q_2=0\}$. By solving the min-max problems

$$\min_{p_1,p_2,q_1,q_2\in C_I}\Big(\max_{k_{min}\le k\le k_{max}}|\rho(k,L,R,\eta,p_1,p_2,q_1,q_2)|\Big), \tag{21}$$

where the index $I\in\{\text{OO0},\text{OO2},\text{2-sided}\}$, we can determine the optimized choice of the parameters in each case. The corresponding optimized transmission conditions are then called OO0 (optimized of order 0), OO2 (optimized of order 2) and 2-sided (two-sided optimized) Robin transmission condition. Using asymptotic analysis, see [3] for details, we obtain for example for OO0 ($q_1=q_2=0$) $p_1=p_2=2^{-1}G_{min}^{\frac{2}{3}}h^{-\frac{1}{3}}$ and $\max_k|\rho_{OO0}|=1-4G_{min}^{\frac{1}{3}}h^{\frac{1}{3}}+O(h^{\frac{2}{3}})$ with overlap $L=h$, and $p_1=p_2=2^{-\frac{1}{2}}G_{min}^{\frac{1}{2}}\pi^{\frac{1}{2}}h^{-\frac{1}{2}}$ and $\max_k|\rho_{OO0}|=1-2^{\frac{3}{2}}G_{min}^{\frac{1}{2}}\pi^{-\frac{1}{2}}h^{\frac{1}{2}}+O(h)$ without overlap. Note that now also the convergence factor depends on the curvature $1/R$ through G_{min}. However, $\lim_{k_{min}\to 0}G_{min}=2\sqrt{\eta}$, independent of R.

4 Comparison of the two families of transmission conditions

We compare now the transmission conditions derived by micro-local analysis to the ones obtained based on optimization. We notice that MATC1 and T0 are identical; MATC5 looks like T2, but without the curvature dependence. In fact, MATC5 is exactly the Taylor condition of order 2 for a straight interface, see [4]. Next, we plot in Fig. 2 all the convergence factors of the Schwarz algorithm (17) with the various transmission conditions for a circular decomposition. We observe that MATC2-4 perform similarly to T2. Since MATC2-4 are of order ≤ 1, we conclude that involving the curvature does improve the performance. It also seems that MATC5 performs quite well. However, this is not always the case: we show a comparison between the three second order transmission conditions in Fig. 3. We can see that MATC5 is much more sensitive to R ($1/R$ is the curvature) than the other two, both in the case

Table 1 Number of iterations required by the Schwarz algorithm with different transmission conditions with overlap $L = h$ and without overlap (in parentheses)

h	Cla	MATC1(T0)	MATC2	MATC3	MATC4	MATC5	T2	OO0	OO2	2-sided
1/50	332	26(310)	20(177)	20(173)	22(208)	17(370)	18(1081)	16(52)	14(48)	41(41)
1/100	684	36(597)	29(354)	27(331)	32(410)	16(644)	23(1832)	21(75)	13(57)	35(51)
1/200	1279	51(1163)	40(662)	39(646)	42(784)	17(1033)	29(3048)	26(101)	14(62)	27(61)
1/400	2919	71(2236)	53(1296)	53(1236)	59(1519)	22(1536)	39(4294)	32(151)	14(70)	23(71)

with and without overlap: the optimized transmission condition performs always better than the other two; the MATC5 gets its best performance around $R = 0.5$ (this is exactly the case of Fig. 2), it performs as T2 at $R = 1$, since then the approximation is identical, and with increasing R it performs worse and worse. We finally note that MATC6 does not perform well: in the middle of Fig. 2, we see that near $k = 1.5$ the convergence factor blows up. Hence MATC6 is not a good choice as transmission condition.

5 Numerical experiments

We perform numerical experiments for a model problem in polar coordinates,

$$\begin{aligned} \partial_{rr}u + \tfrac{1}{r}\partial_r u + \tfrac{1}{r^2}\partial_{\theta\theta}u - \eta u &= f(r,\theta) \text{ in } \Omega, \\ u &= 0 \qquad \text{on } \partial\Omega, \end{aligned} \tag{22}$$

where $\Omega = (0,1)\times(0,2\pi)$ is decomposed into $\Omega = \Omega_1 \cup \Omega_2$, with $\Omega_1 = (0, R+L)\times(0,2\pi)$ and $\Omega_2 = (R,1)\times(0,2\pi)$, and $L \geq 0$ is the overlap. We use a finite difference scheme on a uniform grid with mesh size h to simulate directly the error equations, $f = 0$, for $R = 0.5$ and $\eta = 2$, and a random initial guess is chosen so that all the frequency components are present in the initial error. The number of iterations required by the parallel Schwarz method (17) are shown in Table 1. We clearly see

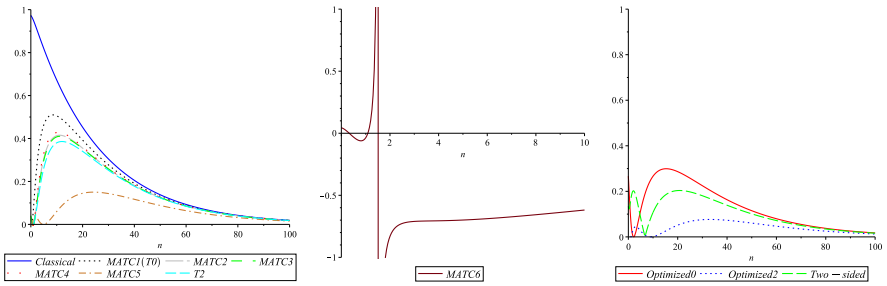

Fig. 2 Convergence factors of MATC1-5 and the Taylor conditions (left), MATC6 (middle), and with optimized transmission conditions (right), for $\eta = 2$, overlap $L = 0.01$ and $R = 0.5$

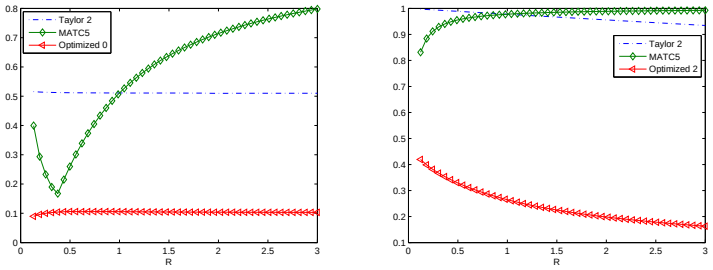

Fig. 3 The maxima of the convergence factors as functions of R with overlap (left) and without (right)

that the transmission conditions based on optimization get better performance in this experiment.

6 Conclusion

We presented two different approaches to take the curvature of interfaces into account in the transmission conditions of optimized Schwarz methods: micro-local analysis, and analysis using a circular model problem. In both cases, we obtained curvature dependent transmission conditions. A preliminary comparison shows that the transmission conditions based on optimization perform better on the model problem, and that it could be important to take the curvature into account in transmission conditions. In our opinion it is however essential to do a more thorough theoretical and numerical study on more general geometry, where micro-local analysis is still applicable, before we can definitely draw conclusions.

References

1. Abramowitz, M., Stegun, I.A.: Handbook of mathematical functions with formulas, graphs, and mathematical tables. Dover pulications, New York (1972)
2. Antoine, X., Barucq, H., Bendali, A.: Bayliss-Turkel-like radiation conditions on surfaces of arbitrary shape. J. Math. Anal. Appl. **229**(1), 184–211 (1999)
3. Barucq, H., Gander, M., Xu, Y.: Optimized Schwarz methods for a reaction-diffusion model with circular domain decomposition. in preparation. (2013)
4. Gander, M.J.: Optimized Schwarz methods. SIAM J. Numer. Anal. **44**(2), 699–731 (2006)
5. Lui, S.H.: A Lions non-overlapping domain decomposition method for domains with an arbitrary interface. IMA J. Numer. Anal. **29**(2), 332–349 (2009)
6. Lui, S.H.: Convergence estimates for an higher order optimized Schwarz method for domains with an arbitrary interface. J. Comput. Appl. Math. **235**(1), 301–314 (2010)